



## Structural characterization and electrocatalytic properties of Au<sub>30</sub>Zr<sub>70</sub> amorphous alloy obtained by rapid quenching

K. BRUNELLI<sup>1,\*</sup>, M. DABALÀ<sup>1</sup>, R. FRATTINI<sup>2</sup> and M. MAGRINI<sup>1</sup>

<sup>1</sup>Dipartimento di Innovazione Meccanica e Gestionale, Università di Padova, via Marzolo 9, 35131 Padova, Italy

<sup>2</sup>INFN-Dipartimento di Chimica Fisica, Università di Venezia, Dorsoduro 2137, 30100 Venezia, Italy

(\*author for correspondence, fax: +39 049 827 5500, e-mail: katya.brunelli@unipd.it)

Received 9 December 2002; accepted in revised form 27 May 2003

**Key words:** activation surface treatments, amorphous alloys, electrocatalysis, formaldehyde, gold, hydrogen evolution reaction, methanol

### Abstract

The present work describes the characteristics of Au<sub>30</sub>Zr<sub>70</sub> amorphous alloy as a precursor of a catalyst for hydrogen evolution both in acid and in basic environments and for oxidation of methanol and formaldehyde in alkaline solutions. Amorphous Au–Zr ribbons were prepared by melt spinning methods and were characterized by X-ray diffraction, optical and scanning electron microscopy. In order to obtain an active electrocatalyst, the surface of the amorphous ribbons was treated by immersion in 1 M HF solution. The results of electrocatalytic tests were compared to those obtained with untreated ribbons and also with electrodes made in polycrystalline pure gold. Moreover, some untreated samples were aged in air for 30 days before the electrochemical measurements, in order to investigate the effect of surface oxidation on the electrochemical behaviour of the alloys. The HF treatment yielded a porous structure rich in nanocrystalline gold particles which had better electrocatalytic activity than untreated ribbons or polycrystalline gold electrodes. Ageing in air produced a duplex phase structure, comprising of ZrO<sub>2</sub> scales and nanocrystalline gold which had also improved electrocatalytic activity.

### 1. Introduction

The demand for new materials exhibiting good electrocatalytic properties, to be employed as alternative to traditional electrodes, has pushed researchers towards the discovery of new compositions and structures. Amorphous alloys have the potential for providing new catalysts (or precursor of catalyst) in many reactions. Specifically electrocatalysis using amorphous alloys as electrodes has been widely studied in a variety of compositions [1–3]. The alloying of metals belonging to early and late transitions groups can generate electronic structures with higher catalytic activity than the single elements [4]. For these reasons, to produce a good catalytic material with high reactivity both in the hydrogen evolution reaction and in oxidation of alcohols and aldehydes, we chose to study an amorphous alloy which oxidizes easily, accompanied with a self-breaking action of the surface oxide layer and constituted by Au and Zr [5]. Gold, which has long been recognized to be poorly active as a catalyst, was recently found to exhibit a surprisingly high activity on various reactions [6]. The surface of melt-quenched amorphous alloys are usually covered by a thin oxide layer which must be removed by chemical etching with HF solution to increase the catalytic activity [7, 8].

In this work we investigated the electrocatalytic activity of amorphous Au<sub>30</sub>Zr<sub>70</sub> alloy both for the hydrogen evolution reaction (in both acid and alkaline environments) and for the oxidation of methanol and formaldehyde reaction in an alkaline environment, were investigated. The effect of an HF activation treatment as well as an oxidation treatment (by aging in air for 30 days) on the structure, surface and electrocatalytic activity is also reported and discussed.

### 2. Experimental details

The amorphous alloy was prepared by melt spinning *in vacuo* at a cooling wheel rate of 3500 cm s<sup>-1</sup>. The specimens, which had composition of Au<sub>30</sub>Zr<sub>70</sub>, were ribbon shaped 1.0–1.2 mm in width and 30 μm in thickness, with apparent surface area of 0.15–0.20 cm<sup>2</sup>, were stored in hydrocarbon in order to prevent the surface oxidation of the alloy. The structure of the alloy was investigated by XRD measurements, performed on a Philips diffractometer with a Bragg–Brentano configuration using a CuK<sub>α</sub> radiation (λ = 154.178 pm (picometre)). The crystalline particle size was determined from the broadening of the diffraction peaks [9]. The surface of the samples was studied on a Cambridge

Stereoscan 440 scanning electron microscope (SEM) equipped with EDS microbeam. To prepare the electrodes for the electrochemical measurements, the specimens were welded to a copper wire which was then sealed into 5 mm diameter Pyrex glass tubing with epoxy resin. The electrodes underwent surface activation treatment by immersion in 1 M HF solution for 30 s and were then rinsed with H<sub>2</sub>O. Some untreated samples were aged in air for 30 days before the electrochemical measurements to investigate the effect of the surface oxidation on the electrochemical behaviour of the alloys. A pure crystalline gold electrode was used as reference electrocatalyst.

Potentiodynamic measurements were performed in both oxygen free 1 M NaOH and 0.5 M H<sub>2</sub>SO<sub>4</sub> solutions with a scanning rate of 1 mV s<sup>-1</sup> to investigate the electrocatalytic activity for the hydrogen evolution. The electrocatalytic activity for the reaction of oxidation of methanol and formaldehyde was achieved by cyclic voltammetry with a scanning rate of 1, 10 and 100 mV s<sup>-1</sup> carried out in 1 M NaOH solutions, containing CH<sub>3</sub>OH (0.5–1.0 M) or HCHO (0.25–1.0 M) at 25 °C under, a stream of nitrogen gas. A Pt electrode and a saturated sulphate electrode (SSE) were used as counter and reference electrodes, respectively. The electrocatalytic activity was evaluated on the basis of apparent unit area of the electrodes.

### 3. Results and discussion

Figures 1 and 2 show the XRD patterns of the as-quenched alloy and of the HF treated alloy, respectively. The amorphous condition of the as-quenched material is clearly revealed. The distance  $a$ , which represents the smallest distance of approach of the atom between a large number of pairs of metallic glass constituents (i.e., the smallest interatomic distance between two atoms) was evaluated by the Ehrenfest relation [10]. A value of 0.1506 nm was obtained for the as-quenched alloy. The activation treatment in 1 M HF gave strong modification in the alloy. The sample surfaces became brittle and Bragg peaks of nanocrystalline gold emerge from the

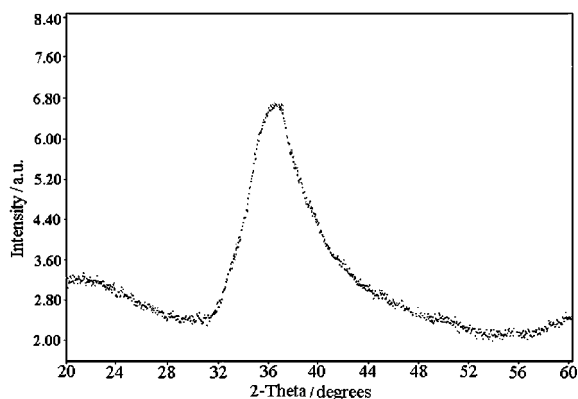


Fig. 1. X-ray diffraction pattern of as-quenched alloy.

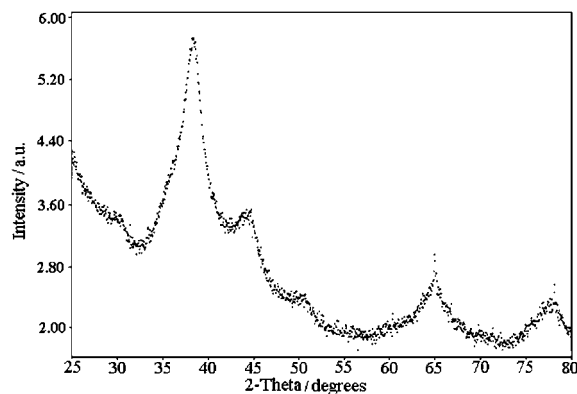


Fig. 2. X-ray diffraction pattern of 1 M HF treated alloy.

amorphous halo. From the line broadening analysis of the Au diffraction peaks, an average particle size of 5 nm was estimated. After aging in air for 30 days the samples darkened and became brittle. As reported in the literature [5], oxidation occurred with formation of crystalline gold and ZrO<sub>2</sub>.

The surfaces of the two sides of the as-quenched alloy showed the characteristics of metallic glasses prepared by melt spinning methods (Figure 3). The inner side had small, parallel grooves due to the contact with the cooling wheel, while the outer side exhibited large randomly located hillocks. Small spherical precipitates of ZrO<sub>2</sub>, with a diameter of about 1 μm, were detected

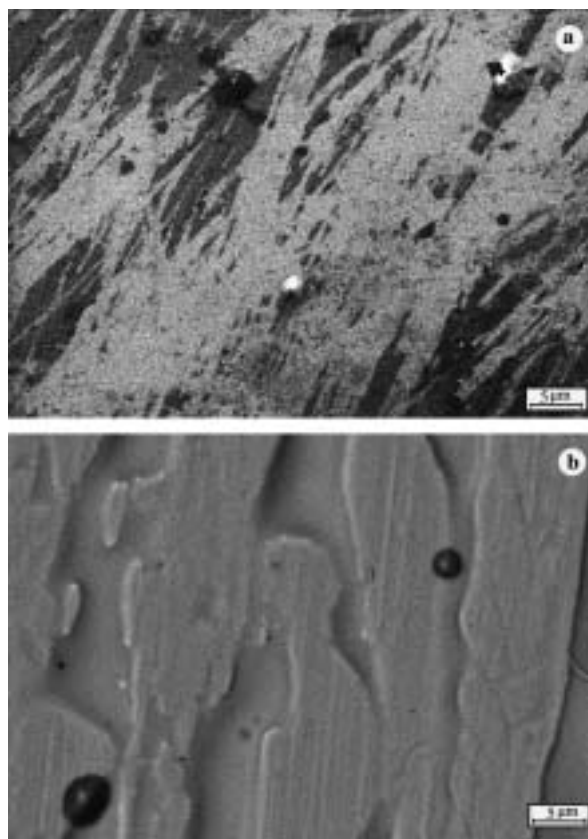


Fig. 3. SEM image of amorphous alloy: (a) outer side and (b) inner side.

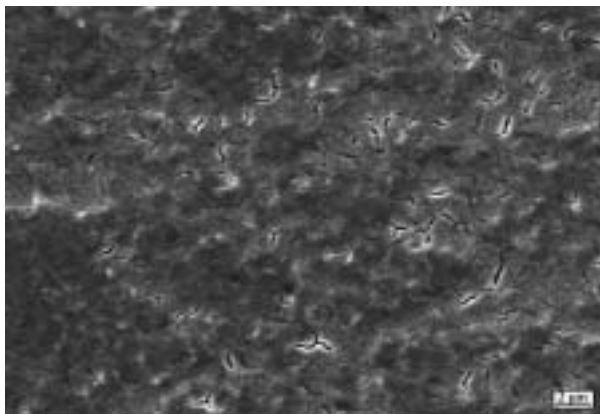


Fig. 4. SEM image of 1 M HF treated alloy surface.

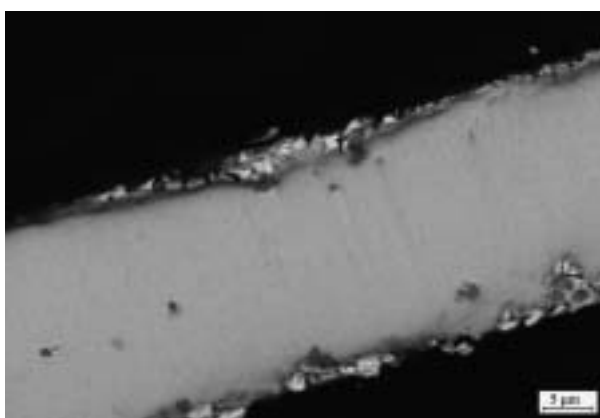


Fig. 5. SEM image of a section of 1 M HF treated alloy.

on both surfaces. The treatment in HF produced a selective dissolution of metallic Zr and  $ZrO_2$  which led to the formation of a porous surface rich in nanocrystalline gold (Figures 4 and 5), as confirmed by EDS analysis. Ageing in air induced the oxidation of the alloy giving rise to duplex phases of  $ZrO_2$  and gold, accompanied by a significant change in volume which embrittled the alloy.

To investigate the electrocatalytic activity for the hydrogen evolution reaction, cathodic polarization tests were carried out in 0.5 M  $H_2SO_4$  and 1 M NaOH solutions and the results are summarized in Figures 6 and 7. The electrocatalytic activity of the samples was compared with that of pure crystalline gold. The polarization curves were used to calculate the cathodic Tafel slope  $b_c$ , which gives information on the reaction mechanism, and the exchange current density  $j_0$ , which can be considered proportional to the catalytic

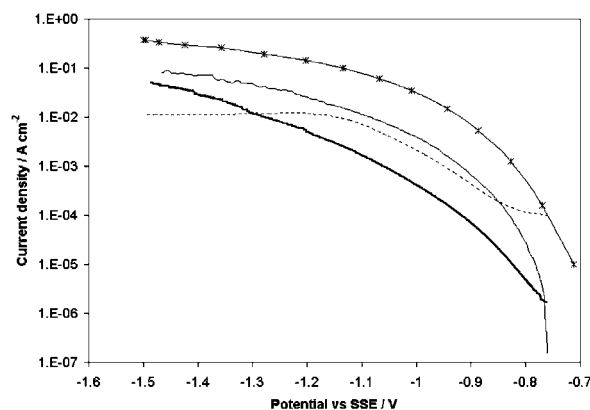


Fig. 6. Cathodic polarization curves measured in  $H_2SO_4$  solutions. Key: (---) Au, (—) aged, (\*—\*) treated and (—) as-quenched.

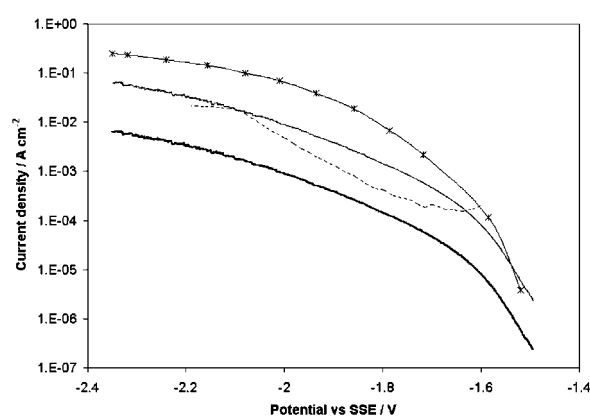


Fig. 7. Cathodic polarization curves measured in NaOH solutions. Key: (---) Au, (—) aged, (\*—\*) treated and (—) as-quenched.

efficiency, extrapolated at the hydrogen reversible potential ( $-0.650$  V vs SSE in acid environment and  $-1.467$  V vs SSE in NaOH solution). The results, reported in Table 1, showed that the electrocatalytic activity of the as-quenched electrodes was lower than pure crystalline gold. In fact, the lowest  $j_0$  values were recorded for the as-quenched electrodes. When the alloy was aged in air for 30 days, the catalytic activity increased until it reached values similar to those of pure crystalline gold. This is because the amorphous structure of the as-quenched alloys changed to a crystalline monoclinic  $ZrO_2$  structure in which nanocrystalline particles of pure fcc gold were dispersed. This structure exhibited higher catalytic activity than as-quenched alloy and crystalline gold probably due to the higher surface area and the presence of more active sites.

The samples treated in 1 M HF showed the highest activity both in acid and alkaline environments because,

Table 1. Electrochemical parameters calculated from polarization curves

Parameters	As quenched		Aged		1 M HF treated		Crystalline Au	
	acid	alkaline	acid	alkaline	acid	alkaline	acid	alkaline
$j_0/A\text{ cm}^{-2}$	$1.20 \times 10^{-7}$	$8.31 \times 10^{-6}$	$3.96 \times 10^{-6}$	$9.96 \times 10^{-5}$	$7.57 \times 10^{-6}$	$5.4 \times 10^{-5}$	$9.96 \times 10^{-7}$	$1.00 \times 10^{-5}$
$b_c/V\text{ dec}^{-1}$	0.125	0.150	0.120	0.150	0.110	0.140	0.120	0.145

as reported in the literature [2, 12, 13], the acid treatment produced higher surface area, as observed by SEM analysis, thus increasing the electrocatalytic activity. However, the increased electrocatalytic activity of the HF treated and aged alloy could be ascribable, in addition to the higher surface area, to a hybridization of the d-orbitals of Zr and gold which produced a bond weakening between the alloy and hydrogen, causing a faster catalytic hydrogen reduction reaction [12]. The cathodic Tafel slope  $b_c$  varied from  $120 \text{ mV dec}^{-1}$  in acid environment to  $150 \text{ mV dec}^{-1}$  in alkaline environment, typical values for hydrogen evolution reactions. This indicates that the reaction mechanism of the hydrogen evolution was the same for all samples and the change between acid and basic environments and between HF treated electrodes and the untreated ones, and is not attributable to a variation in the reaction mechanism but, more likely, to a modification of the surface area of the electrodes [13]. Further studies are in progress to clarify the effect of the increased surface area and of the surface electronic structure on the catalytic behaviour. Moreover, for potential values more negative than  $-1.2 \text{ V}$  vs SSE in acid environment and  $-2 \text{ V}$  vs SSE in alkaline environment, the cathodic curves showed an asymptotic trend due to the formation of hydrogen bubbles on the surface, which decreased the reaction rate. This effect was more evident on both the HF treated and aged electrodes because the porous nature of the surfaces may have produced an ohmic drop due to the occlusion of gas in pores [12].

The electrocatalytic activity of the  $\text{Au}_{30}\text{Zr}_{70}$  alloy for the reaction of oxidation of methanol was investigated in  $1 \text{ M NaOH}$  solutions containing various amount of methanol. Figure 8 summarizes the cyclic voltammograms of HF treated materials. No activity was detected in  $1 \text{ M NaOH}$  environment except for a cathodic peak at about  $-0.6 \text{ V}$  in the reverse sweep related to the surface gold oxide reduction. An anodic peak with a maximum at about  $-0.2 \text{ V}$  was recorded in methanol containing solutions. The current density of the peak increased with the concentration of methanol and could be ascribable

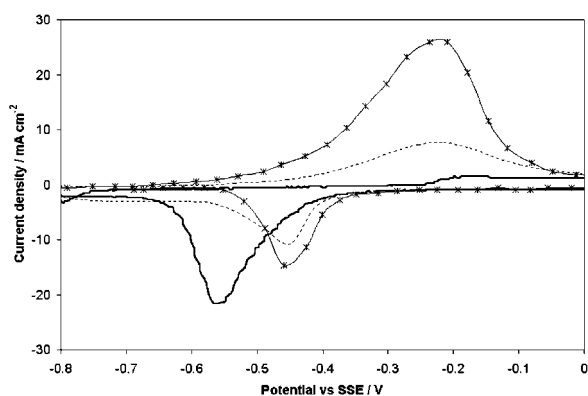


Fig. 8. Cyclic voltammograms of  $1 \text{ M}$  HF treated amorphous alloy measured in  $1 \text{ M NaOH}$  containing various amount of  $\text{CH}_3\text{OH}$  at a sweep rate of  $10 \text{ mV s}^{-1}$ . Key: (---)  $0.5 \text{ M}$  methanol, (—)  $1 \text{ M NaOH}$  and (\*—\*)  $1 \text{ M}$  methanol.

to the oxidation of methanol reaction. However, the oxidation of the surface, which was covered by the reaction products, decreased the electrocatalytic activity and caused the subsequent reduction in current density after the maximum. A similar behaviour was observed with pure crystalline gold electrodes [14, 15], even if the treated material showed a current density, measured at maximum, about three orders of magnitude higher than gold due to the surface enrichment in gold and the porosity caused by HF. This suggests that the reaction mechanism for methanol oxidation was the same in the amorphous materials and in pure crystalline gold, since the active species on the electrodes was the same.

Figure 9 shows the voltammograms of an HF treated electrode in  $1 \text{ M NaOH}$  containing  $1 \text{ M CH}_3\text{OH}$  solutions at various sweep rates. The higher catalytic activity of the treated samples than the as-quenched electrodes was ascribable to the increased surface area, as in the case of the hydrogen reduction reaction, and especially to the presence of nanostructured Au particles with mean size of  $5 \text{ nm}$ , as observed by SEM and XRD data. It has been shown that nanostructured catalysts with size of  $5 \text{ nm}$  or less showed unique catalytic properties [16–18]. For a sweep rate of  $1 \text{ mV s}^{-1}$  a methanol oxidation anodic peak in the reverse sweep was observed. During the reverse sweep, the reduction of surface oxides which deactivated the electrode surface allowed the reactivation of the electrode and therefore the methanol oxidation. For higher sweep rate, there was not enough time to reduce these compounds, so that the reactivation of the electrode did not occur and this effect was not present. The electrocatalytic activity of the aged electrode was higher than as-quenched electrode but lower than HF treated electrode. This was related to the surface modification that occurred during ageing in air which increased the porosity of the alloy and induced the formation of a duplex phase of  $\text{ZrO}_2$  and crystalline gold.

Figure 10 shows the current density measured at the peak maximum against the  $\text{CH}_3\text{OH}$  concentration in a  $0.5 \text{ M NaOH}$  solution for the HF treated electrode. The

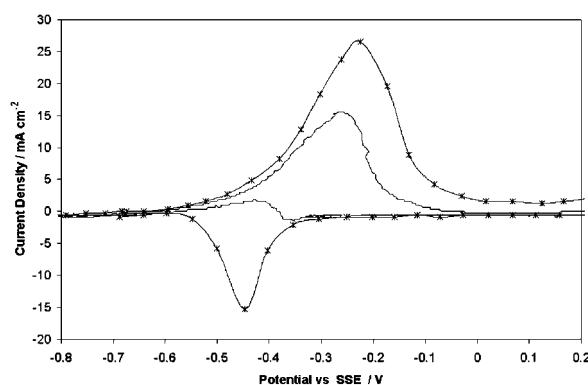


Fig. 9. Cyclic voltammograms of  $1 \text{ M}$  HF treated amorphous alloy measured in  $1 \text{ M NaOH}$  containing  $1 \text{ M CH}_3\text{OH}$  at different sweep rate. Key: (—)  $1 \text{ mV s}^{-1}$  and (\*—\*)  $10 \text{ mV s}^{-1}$ .

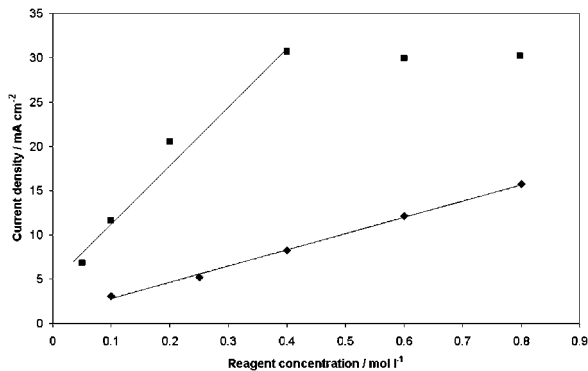


Fig. 10. Influence of methanol concentration in a solution 0.5 M NaOH and of NaOH concentration in a solution 1 M CH<sub>3</sub>OH on the current density measured at the peak maximum. Key: (◆) methanol and (■) NaOH.

current density increased proportionally to the methanol concentration, suggesting a first order reaction for methanol, as observed for pure crystalline gold electrodes [14]. Moreover, the current density increased proportionally with the base concentration up to 0.5 M, while for higher concentrations no change of current density was recorded, because the electrodes were saturated with OH<sup>-</sup> ions [14]. In any case, a first order reaction for NaOH was observed for concentrations lower than 0.5 M.

The electrocatalytic activity of the Au<sub>30</sub>Zr<sub>70</sub> glassy metal was investigated in 1 M NaOH solutions containing various amount of HCHO. At all HCHO concentrations for the HF treated electrodes, the reaction started at approximately -1.5 V during the anodic sweep and ended at the same potential during the reverse sweep, (Figure 11). In most cases, on the anodic sweep the current rose to a plateau ascribable to a diffusion-controlled step of the oxidation reaction, while at high potentials a drop of the current was observed associated with the monolayer oxide deactivation of the electrode surface. However, for formaldehyde concentrations lower than 0.1 M, a further increase of the current at approximately -0.2 V was recorded. This

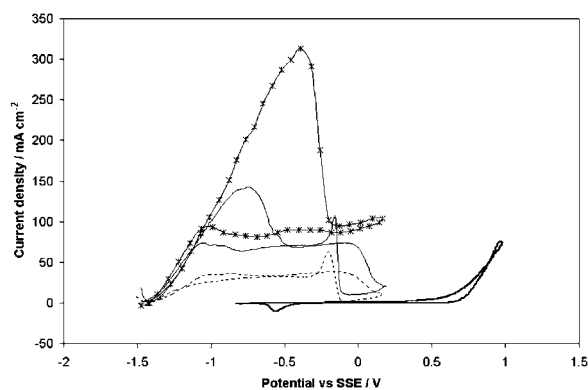


Fig. 11. Cyclic voltammograms of 1 M HF treated alloys measured in 1 M NaOH containing various amount of HCHO at a sweep rate of 10 mV s<sup>-1</sup>. Key: (—) 1 M NaOH, (- - -) 0.25 M formaldehyde, (· · ·) 0.5 M formaldehyde and (\*—\*) 1 M formaldehyde.

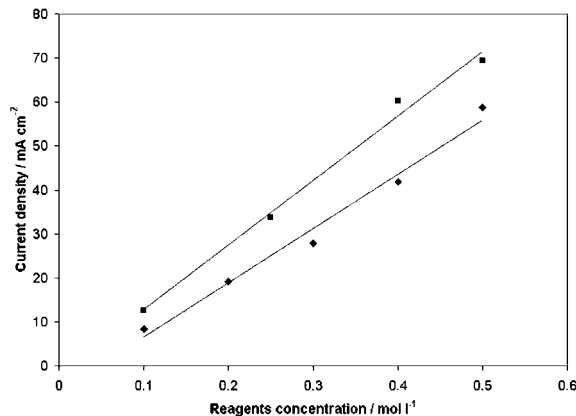


Fig. 12. Influence of NaOH and formaldehyde concentration on the plateau current density. Key: (◆) NaOH and (■) HCHO.

behaviour has been observed for pure gold electrodes and was due to the intervention of a new surface redox couple [19]. On the reverse sweep, the oxide layer was removed and the surface reactivated, thus causing a vigorous formaldehyde oxidation with the appearance of a peak at about -0.2 V. The subsequent drop of the current in the reverse sweep to about the value of plateau current recorded during the anodic sweep indicated a diffusion-controlled reaction. However, a high oxidation current was observed in the reverse sweep at potentials lower than -0.5 V, especially for high formaldehyde concentrations. This was due to the reduction of some Au(III) hydrous oxide sites [19]. As reported in Figure 12, the plateau current for the anodic sweep of the HF treated electrodes was a linear function of both NaOH and formaldehyde concentration, at least up to 0.5 M HCHO. This was in agreement with the suggested mechanism of formaldehyde oxidation reaction on pure gold electrodes, indicating that the rate determining step of aldehyde oxidation involved the cleavage of a carbon-hydrogen bond on Au(I) hydrous oxide species [19].

#### 4. Conclusions

The Au<sub>30</sub>Zr<sub>70</sub> amorphous alloy obtained by melt spinning is a material which can be considered a precursor for using as an electrode in the electrocatalysis of hydrogen evolution reaction and in the oxidation of alcohols and aldehydes. The evaluation of the electrocatalytic activity showed that interesting electrocatalytic performances in all the investigated reactions were obtained after chemical etching of the ribbons in HF solution and after ageing in air. Indeed, the treated materials exhibited higher current densities than both as-quenched materials and pure crystalline gold electrodes. Structural and morphological characterizations of the amorphous alloy showed that the increase in electrocatalytic activity was mainly the consequence of surface structure modifications. The treatment in HF

dissolved selectively metallic Zr and the ZrO<sub>2</sub> from the surface, leading to the formation of a porous surface rich in nanocrystalline gold particles, while ageing in air induced an oxidation of the alloy which changed the structure from amorphous to duplex phases of ZrO<sub>2</sub> and gold, accompanied by a significant change in volume. The higher catalytic activities of the treated electrodes were ascribable to the increased surface area and to the presence of nanostructured Au particles.

## References

1. M.D. Archer, C. Corke and B.H. Harji, *Electrochim. Acta* **32** (1987) 13.
2. A. Molnar, G.V. Smith and M. Bartok, *Adv. Catal.* **36** (1989) 329.
3. Y. Hayakawa, A. Kawashima, H. Habazaki, K. Asami and K. Hashimoto, *J. Appl. Electrochem.* **22** (1992) 1017.
4. M.M. Jaksic, *J. Mol. Catal.* **38** (1986) 161.
5. H. Kimura, A. Inoue, T. Masumoto and S. Itabashi, *Sci. Rep. RITU A* **33** (1986) 183.
6. M. Haruta, A. Ueda, S. Tsubota and R.M. Torres Sanchez, *Catal. Today* **29** (1996) 443.
7. K. Brunelli, M. Dabalà, R. Frattini, G. Sandonà and I. Calliari, *J. Alloy Compd.* **317–318** (2001) 595.
8. K. Brunelli, M. Dabalà and M. Magrini, *J. Appl. Electrochem.* **32** (2002) 145.
9. S. Enzo, R. Frattini, R. Gupta, P.P. Macri, G. Principi, L. Schiffini and G. Scipione, *Acta Mater.* **44** (1996) 1786.
10. A. Guinier, H.M. Fowley and M.A. Ruderman (Eds), 'X-ray Diffraction in Crystals, Imperfect Crystals and Amorphous Bodies' (W.H. Freeman, San Francisco, 1963), p. 61.
11. S. Trasatti, *J. Electroanal. Chem.* **39** (1972) 63.
12. M. Metikos-Hukovic and A. Jukic, *Electrochim. Acta* **45** (2000) 4159.
13. S. Spriano, M. Baricco, C. Antonione, E. Angelini, F. Rosalbino and P. Spinelli, *Electrochim. Acta* **39** (1994) 1781.
14. E. Gonzalez Hernan, C. Alonso and J. Gonzalez-Velasco, *J. Appl. Electrochem.* **17** (1987) 868.
15. M. Avramov-Ivic, V. Jovanovic, G. Vlajnic and J. Popic, *J. Electroanal. Chem.* **423** (1997) 119.
16. M.L. Trudeau and J.Y. Ying, *Nanostructured Mater.* **7** (1996) 245.
17. J. Luo, M.M. Maye, Y. Luo, L. Han, M. Hapel and C.J. Zhong, *Catal. Today* **77** (2002) 127.
18. C.W. Corti, R.J. Holliday and D.T. Thompson, *Gold Bulletin* **35** (2002) 111.
19. L.D. Burke and W.A. O'Leary, *J. Appl. Electrochem.* **19** (1989) 758.